Application of Fresnel diffraction from a phase step to the measurement of film thickness

Mohammad Taghi Tavassoly,* Iman Moaddel Haghighi, and Khosrow Hassani
Department of Physics, University of Tehran, Kargar Shomally Avenue, Tehran 14394-547, Iran
*Corresponding author: tavasoli@iasbs.ac.ir

Received 15 June 2009; revised 13 September 2009; accepted 14 September 2009;
posted 15 September 2009 (Doc. ID 112798); published 1 October 2009

When a thin film that is prepared in a step form on a substrate and coated uniformly with a reflective material is illuminated by a parallel coherent beam of monochromatic light, the Fresnel diffraction fringes are formed on a screen perpendicular to the reflected beam. The visibility of the fringes depends on film thickness, angle of incidence, and light wavelength. Measuring visibility versus incident angle provides the film thickness with an accuracy of a few nanometers. The technique is easily applicable and it covers a wide range of thicknesses with highly reliable results.

OCIS codes: 050.1960, 120.5050, 120.3940, 260.1960.

1. Introduction

Film thickness is an important parameter in thin-film technology and devices [1]. Therefore, a large number of methods have been introduced for measuring film thickness in different conditions and ranges [2–6]. Among these methods, those based on the interference of light (two beam and multiple beam) are more frequently used [7,8]. In these methods, the film is prepared in the shape of a step or channel on a plate. Then, using another transparent or semitransparent plate, the wedge fringes are studied with a low-magnifying microscope. The accuracies of these techniques depend on the precision with which the fringe spacing is measured. In two-beam interferometry, in practice, it is difficult to measure a film thickness with an accuracy of better than $\lambda/30$ (λ is the light wavelength) [3]. In a multiple-beam technique, higher accuracy is possible, but careful sample preparation is required [8–10]. The main shortcomings of these techniques are limited thickness range, dependence of the accuracy on the flatness of the wedge planes, and intensity fluctuations [9,10]. Also, white-light interferometry and ellipsometry are often used for film thickness measurement [11–13]. But, the former does not work for very thin films and usually is applied to transparent films. The latter is not applicable to thick opaque films and is very sensitive to contamination.

In a technique that is introduced in this report, the criterion of thickness measurement is the visibility of the Fresnel fringes formed by a step of height equal to the film thickness. The visibility can vary from zero to 1 for a thickness change of $\lambda/4$. In addition, since the optical path difference of the light diffracted from the two sides of the step edge varies as the incident angle changes and the fringe visibility versus incident angle is a known universal function, fitting the latter function on experimentally obtained visibilities in a range of incident angles provides the film thickness very accurately.

2. Theoretical Considerations

In Fig. 1 the cylindrical wavefront Σ incidents to a step of height h. The symmetry axis of the wavefront that passes through point S is parallel to the step edge. By using the Fresnel–Kirchohoff integral, the diffracted amplitude and intensity can be calculated at point P, on line $S'P$, where S' is the mirror image of S. The intensity at point P depends on the location of P_0, the origin of the coordinate system used for the intensity calculation at point P. In fact; the point P_0 is the intersection point of the line $S'P$ and the

0003-6935/09/295497-05$15.00/0

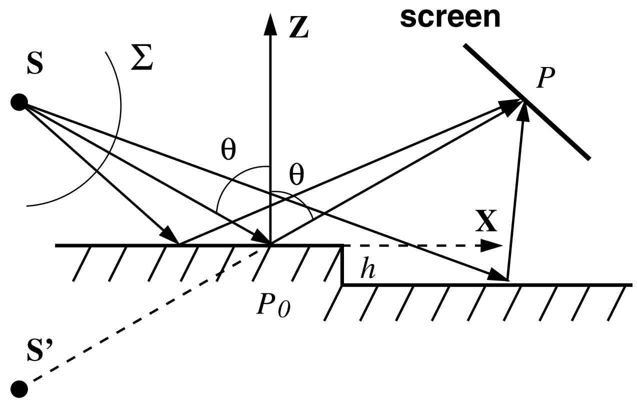

Fig. 1. Geometry used to show the Fresnel diffraction from a one-dimensional (1D) step.

step profile. For a plane wave, that is, source at infinity, the point P_0 is the intersection point of the step and normal to the screen at point P. For point P_0 on the left side of the step edge and the given coefficients of the amplitude reflection r_L and r_R, for the left and right sides of the step edge, the intensity at point P is given by [14]

$$\begin{aligned} I_L = {} & I_0 r_L r_R [\cos^2(\varphi/2) + 2(C_0^2 + S_0^2)\sin^2(\varphi/2) \\ & - (C_0 - S_0)\sin\varphi] \\ & + \frac{I_0}{2}[(1/2 + C_0^2 + S_0^2)(r_L - r_R)^2 \\ & + (C_0 + S_0)(r_L^2 - r_R^2)], \end{aligned} \tag{1}$$

where I_0 is proportional to the illuminating intensity, $\varphi = 4\pi h \cos\theta/\lambda$ is the phase introduced by the step (θ stands for the incident angle at point P_0), and C_0 and S_0 represent the well-known Fresnel cosine and sine integrals associated with the distance between P_0 and the step edge, respectively. For $r_L = r_R$, uniform reflectance across the step, the normalized intensity at a point on the left or right side of the edge, specified by − and +, respectively, is expressed as [14,15]

$$\begin{aligned} I_n = {} & [\cos^2(\varphi/2) \\ & + 2(C_0^2 + S_0^2)\sin^2(\varphi/2) \mp (C_0 - S_0)\sin\varphi]. \end{aligned} \tag{2}$$

The plots of Eq. (2) for (a) $h = \lambda/12$, (b) $h = \lambda/4$, and (c) $h = 3\lambda/7$, versus the location of point P_0, are illustrated in Fig. 2. As the plots show, the visibility of the fringes varies with h and with the distance from the step edge. Now, to provide a quantitative measure for the contrast of the fringes, we define the visibility for the three central fringes as

$$V = \frac{\frac{I_{\max L} + I_{\max R}}{2} - I_{\min}}{\frac{I_{\max L} + I_{\max R}}{2} + I_{\min}}, \tag{3}$$

where $I_{\max L}$ and $I_{\max R}$ stand for the maximum intensities of the left- and right-side bright fringes, while $I_{\min}$ represents the minimum intensity of the central dark fringe. Equation (3) versus the optical path difference divided by wavelength ($\Delta/\lambda = \varphi/2\pi$) is plotted in Fig. 3. According to Fig. 3, as the optical path difference changes by $\lambda/2$, which is equivalent to the change of film thickness by $\lambda/4$ in reflection, the visibility varies from zero to 1.

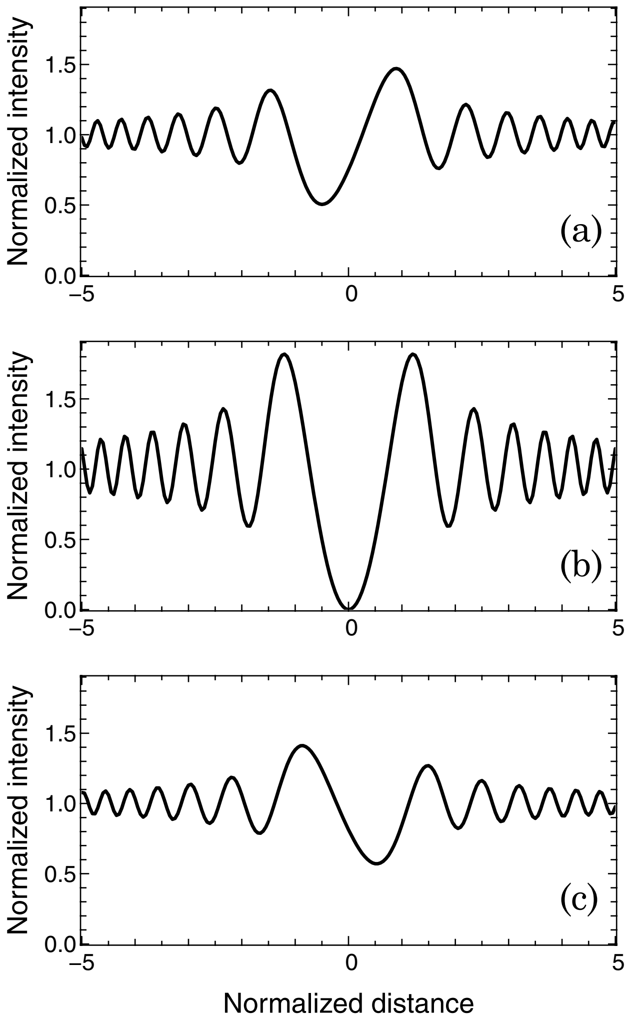

Fig. 2. Calculated normalized intensity distribution on the diffraction patterns of lights diffracted from a 1D step of height (a) $\lambda/12$, (b) $\lambda/4$, and (c) $3\lambda/7$.

We should also emphasize that the curve in Fig. 3 is a universal curve for any step with the same reflectance on both sides of the step edge. Thus, by fitting experimentally obtained visibilities on such a curve, one can obtain the step height or the film thickness. Also, according to Fig. 3, when the visibility is less than 0.7, in other words, for $\Delta/\lambda < 0.25$ and $\Delta/\lambda > 0.75$, the visibility values fit neatly on two straight lines that make angles $\alpha = \tan^{-1} 2.77$ and $\alpha = (\pi - \tan^{-1} 2.77)$ with the horizontal axis. Thus, these lines can be used for film thickness measurement. However, since by changing the incident angle, it is always possible to shift the optical path difference into the mentioned regions, the plotted lines can be exploited for any film thickness measurement. This is a remarkable advantage to derive the film

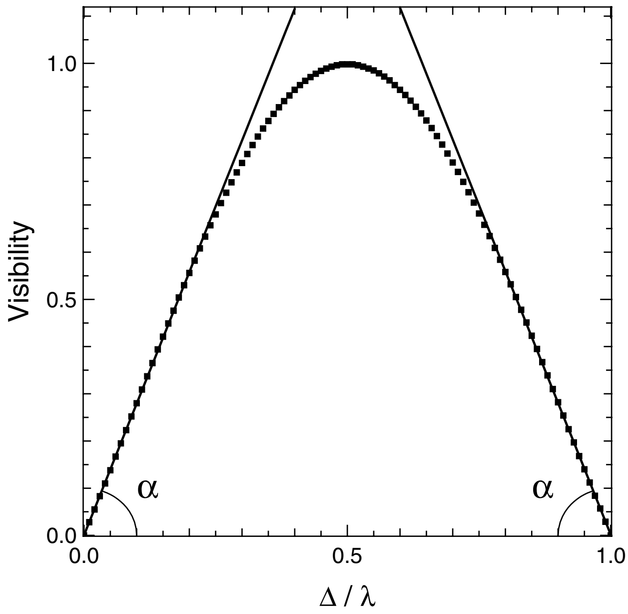

Fig. 3. Calculated visibility of the three central diffraction fringes formed by the light diffracted from a 1D step, versus the optical path difference divided by the wavelength, Δ/λ. The visibilities under 0.7 lie on the linear parts of the visibility curve.

thickness from a linear function. In practice, we measure the visibilities in a suitable interval of incident angles and find the slope of the best-fitted line and equate it to that of the calculated one in the following way. Recalling that $\Delta = 2h\cos\theta$, for the line on the left side of Fig. 3 we can write

$$\tan\alpha = \frac{(V_2 - V_1)\lambda}{2h(\cos\theta_2 - \cos\theta_1)}, \tag{4}$$

where V_2 and V_1 are visibilities at incident angles θ_2 and θ_1. Substituting $(V_2 - V_1)/(\cos\theta_2 - \cos\theta_1)$ by the experimentally obtained slope, s and $\tan\alpha$ by 2.77, we get

$$h = \frac{s\lambda}{5.54}. \tag{5}$$

Plotting a straight line with many points assures the reliability of the results. Since s in Eq. (5) can have almost any value practically, there is no restriction on film thickness. It should be mentioned that the presented technique provides the average film thickness on the strip adjacent to the step edge, not the average thickness of the entire film. In addition, for large thicknesses, it is required to increase the distance between the step and the screen in order to increase the effective area of the diffractor. Therefore, a wider incident wavefront is required and nonuniformity in the initial phase distribution causes error in thickness measurement.

3. Experimental Procedure and Results

First, we coat a film on a partly masked glass slide (by evaporation in vacuum). Then we remove the mask and get the required step. By coating both sides of the step with a reflective material, for example, aluminum, we get a step with the same reflectance on both sides. We install the slide on a stand that can rotate horizontally and illuminate it with an expanded parallel laser beam (Fig. 4). We mount a CCD on an arm that can turn around the axis of the stand. The CCD is connected to a personal computer through a frame grabber card. In the setup we used, the diameter of the laser beam was 30 mm and the incident angle could be varied by the accuracy of 1 arcmin. A commercial CCD (Topica, TP1001) was mounted at a distance of 100 mm from the slide. By rotating the holder of the slide, the incident angle is changed and CCD facing the reflected beam records the diffraction pattern.

Figure 5 illustrates three typical experimental diffraction patterns formed by steps and the corresponding intensity profiles averaged along the lines parallel to the step edge. The pattern was obtained by diffracting a He–Ne laser beam from a step formed by a film of thickness of 446 nm and coated entirely by aluminum film, at incident angles (a) 56°, (b) 68°, and (c) 77°. The dots are experimental data. In Fig. 6, the experimental visibilities (triangles) of the three central fringes defined by Eq. (3) versus the cosine of the incident angle are plotted for a step formed by an aluminum film of thickness 446 nm. The solid curve is the theoretically calculated visibility.

In Fig. 7 the circles and triangles are experimental visibilities, for wavelengths $\lambda = 633$ nm and $\lambda = 532$ nm, respectively, versus the cosine of the incident angle in the linear part of the visibility curve for a film thicknesses of (a) 57 nm and (b) 462 nm. The solid lines are the best-fitted visibility lines. To obtain the thickness of a film, we measure the slope of the experimental visibility line and substitute it into Eq. (5).

Six different film thicknesses, listed in Table 1, have been measured by this method, using two different wavelengths. Also, the standard deviations for about 50 measurements for each thickness are given in the table. The accuracy of the thickness

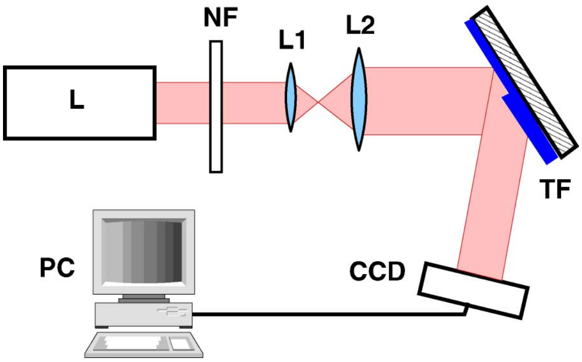

Fig. 4. (Color online) Sketch of the experimental setup. L, NF, L1, L2, TF, CCD, and PC stand for laser, neutral filter, lenses 1 and 2, thin film with step, intensity detector, and personal computer, respectively.

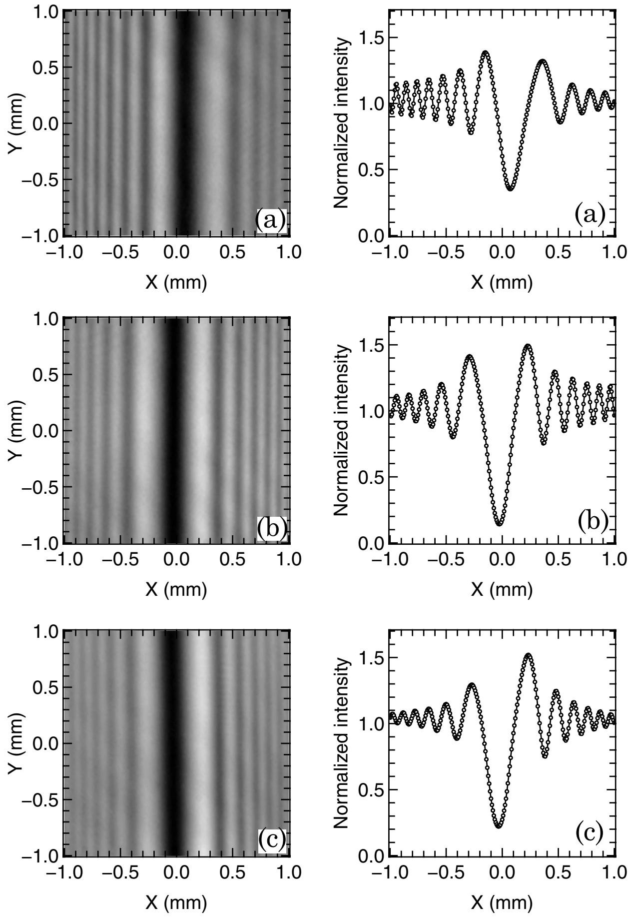

Fig. 5. Typical experimental diffraction patterns and intensity profiles of lights diffracted from a step formed by a thin film of thickness 446 nm at incident angles (a) 56°, (b) 68°, and (c) 77°. The dots are experimental values averaged over the lines parallel to the step edge. The light wavelength was $\lambda = 632.8\,\mathrm{nm}$.

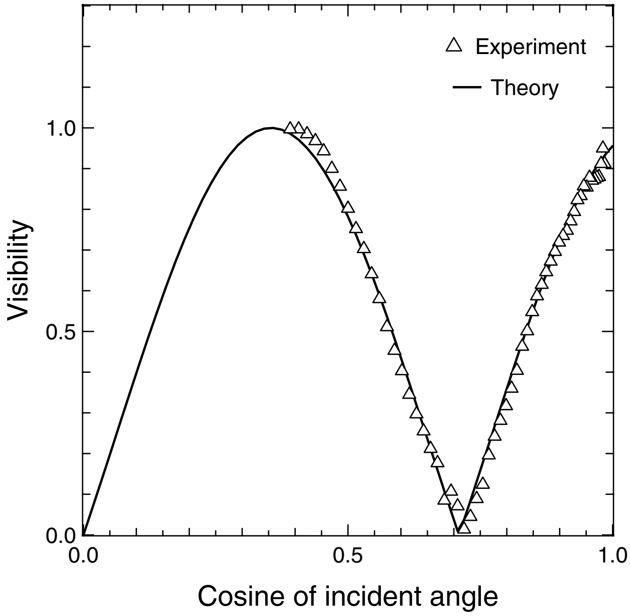

Fig. 6. Experimental visibilities, Δ, versus the cosine of incident angle for the three central diffraction fringes of light diffracted from a step formed by a thin film of thickness 446 nm. The solid curve is the calculated visibility.

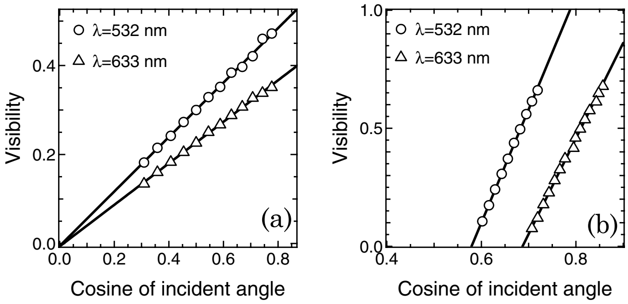

Fig. 7. Circles and triangles are experimental visibilities for the incident light wavelengths $\lambda = 532\,\mathrm{nm}$ and $\lambda = 633\,\mathrm{nm}$, respectively, versus the cosine of incident angle in the linear part of the visibility curve for film thicknesses of (a) 57 nm and (b) 462 nm. The solid lines are the best fitted visibility lines.

measurement depends on the precision with which the visibility can be evaluated. A visibility change of 1% is equivalent to $\lambda/400$ in thickness. Thus, in principle; an accuracy of the order of nanometers is accessible. But, in practice, the error in incident angle measurement, in detector reading, in flatness of the substrate, in homogeneity of the film and the step's coating, and fluctuations in light intensity affect the accuracy of the measurement. Thus, the statistically calculated error provides a fair estimation of the measurement accuracy. The measurable lower limit of film thickness depends very sensitively on the quality of the substrate, film, detector, and also on fluctuations of the light source. In our study, we did not try thicknesses less than 30 nm. But, for the upper limit in another work, we have measured the optical thickness, nh, of transparent plates of millimeters of physical thickness.

To check the results in another way, we recall that, according to Fig. 3, for a film thickness or step height larger than $\lambda/4$, at certain incident angles, that is, at angles for which $h\cos\theta = m\lambda/2$, $m = 1, 2, \ldots$, the visibility becomes zero. Thus, for $m > 1$, by finding two successive incident angles for which the visibilities are zero, one can directly calculate the film thickness from the following equation:

$$h = \frac{\lambda}{2(\cos\theta_1 - \cos\theta_2)}. \tag{6}$$

Table 1. Six Film Thicknesses Measured Using Fresnel Diffraction of Light from Steps Formed by the Thin Films Using Two Different Wavelengths

No.	Film Thickness in nm for $\lambda = 532\,\mathrm{nm}$	Film Thickness in nm for $\lambda = 633\,\mathrm{nm}$	Standard Deviation in nm for $\lambda = 532\,\mathrm{nm}$	Standard deviation in nm for $\lambda = 633\,\mathrm{nm}$
1	466	465	6.5	5.9
2	444	446	6.5	5.5
3	239	242	4.8	4.1
4	80	82	3.9	6.1
5	57	55	2.1	2.4
6	39	40	1.5	2

Table 2. Comparison between the Thicknesses Measured by Fitting Data on Visibility Line (FVL) and the Thicknesses Obtained from Zero Visibility Point (ZVP)

FVL	466 ± 6.5 nm	465 ± 5.9 nm	444 ± 6.5 nm	446 ± 5.5 nm
ZVP	454 ± 20 nm	457 ± 20 nm	436 ± 20 nm	438 ± 20 nm

Applying this technique, we repeated the measurement for some of the thicknesses listed in Table 1. The results are given in Table 2 for comparison. The thicknesses obtained by fitting the visibilities on the visibility line and by specifying the zero visibility point are denoted by FVL and ZVP, respectively.

Finally, we should mention that the application of this technique in transmission can provide the optical path difference imposed by the step, that is, nh, where n is the film refractive index. Thus, Fresnel diffraction in reflection and transmission from a transparent film prepared in a step shape can provide the thickness and the refractive index of the film.

4. Conclusion

This study shows that Fresnel diffraction from a phase step provides a reliable and easily applicable method for measuring film thickness with the following advantages.

a. It covers a wide range of thicknesses, from several nanometers to several micrometers, with an accuracy of a few nanometers using simple optics.

b. Since the film thickness is obtained by fitting experimental data on a linear function, the accuracy of the measurement and the reliability of results is very high.

c. Application of the technique to a transparent film in reflection and transmission modes provides the film thickness and its refractive index.

References

1. K. L. Chopra, *Thin Film Phenomena* (McGraw-Hill, 1969).
2. H. K. Pulker, “Film thickness,” in *Coating On Glass* H. K. Pulker, ed. (Elsevier, 1984), pp. 287–340.
3. W. A. Pliskin and S. J. Zanin, “Film thickness and composition,” in *Handbook of Thin Film Technology* L. I. Maissel and R. Glang, eds. (McGraw-Hill, 1970), pp. 11:1–11:54.
4. “Film thickness,” in *Semiconductor Measurements and Instrumentation*, W. R. Runyan and T. J. Shaffner, eds. (McGraw-Hill, 1998), pp. 177–199.
5. D. M. Mattox, “Non-elemental characterization of films and coatings,” in *Handbook of Deposition Technologies for Films and Coatings*, R. F. Bunshah, ed. (Noyes, 1994).
6. L. Eckertová, *Physics of Thin Films* (SNTL, 1986).
7. S. Tolansky, *Multiple Beam Interferometries* (Clarendon, 1948).
8. C. Weaver and P. Benjamin, “Measurement of the thickness of thin films by multiple-beam interference,” Nature **177**, 1030–1031 (1956).
9. O. S. Heavens, “Measurement of the thickness of thin films by multiple-beam interferometry,” Proc. Phys. Soc. B **64**, 419–425 (1951).
10. C. Weaver and P. Benjamin, “Errors in the measurement of film thickness by multiple-beam interferometry,” Nature **182**, 1149–1150 (1958).
11. K. Seung-Woo and K. Gee-Hong, “Thickness-profile measurement of transparent thin-film layers by white-light scanning interferometry,” Appl. Opt. **38**, 5968–5973 (1999).
12. P. Hlubina, J. Lunacek, and D. Ciprian, “White-light spectral interferometry and reflectometry to measure thickness of thin films,” Proc. SPIE **7389**, 738926 (2009).
13. A. Franquet, J. De Laet, T. Schram, H. Terryn, V. Subramanian, W. J. van Ooij, and J. Vereecken, “Determination of the thickness of thin silane films on aluminium surfaces by means of spectroscopic ellipsometry,” Thin Solid Films **384**, 37–45 (2001).
14. M. T. Tavassoly, M. Amiri, A. Darudi, R. Alipour, A. Saber, and A.-R. Moradi, “Optical diffractometry,” J. Opt. Soc. Am. A **26**, 540–547 (2009).
15. M. Amiri and M. T. Tavassoly, “Fresnel diffraction from 1D and 2D phase steps in reflection and transmission modes,” Opt. Commun. **272**, 349–361 (2007).